

## Band structure in $^{80}\text{Kr}$

D. L. Sastry,\* A. Ahmed,<sup>†</sup> A. V. Ramayya, R. B. Piercey, H. Kawakami,<sup>‡</sup> R. Soundranayagam, J. H. Hamilton, C. F. Maguire, A. P. de Lima,<sup>§</sup> and S. Ramavataram

*Physics Department, Vanderbilt University, Nashville, Tennessee 37235*

R. L. Robinson and H. J. Kim

*Oak Ridge National Laboratory, Oak Ridge, Tennessee 37830*

J. C. Wells

*Physics Department, Tennessee Technological University, Cookeville, Tennessee 38501*

(Received 24 November 1980)

The levels of  $^{80}\text{Kr}$  have been investigated using in-beam  $\gamma$ -spectroscopy techniques via the  $^{70}\text{Zn}(^{12}\text{C}, 2n)^{80}\text{Kr}$  reaction with 38.4 MeV  $^{12}\text{C}$  ions. The energies, relative intensities, and angular distributions of the  $\gamma$  rays were measured. The proposed level scheme shows four bands: three of even parity and one of odd parity. Two-quasiparticle-plus-rotor calculations for  $^{80}\text{Kr}$  suggest that the even-parity band built on the  $(8^+)$  state at 3701.6 keV has primarily a proton  $(g_{9/2})^2$  configuration and the odd-parity band built on the  $5^-$  state at 2861.0 keV has an essentially pure two-quasiproton  $(f_{5/2}, g_{9/2})^2$  configuration. The observed backbending in the yrast band is attributed to the crossing of the ground band and the excited positive-parity band.

[NUCLEAR REACTIONS  $^{70}\text{Zn}(^{12}\text{C}, 2n)$ ,  $E=33.0\text{--}38.4$  MeV; measured  $E_\gamma$ ,  $I_\gamma$ ,  $\gamma(\theta)$  DCO; deduced  $^{80}\text{Kr}$  levels,  $J$ ,  $\pi$ , and  $\gamma$  branching; performed two-quasiparticle-plus-rotor model calculations.]

### I. INTRODUCTION

In the course of our systematic study of even-even nuclei in the mass region around  $A=70$ , we have studied the nuclear structure of  $^{80}\text{Kr}$  via the  $^{70}\text{Zn}(^{12}\text{C}, 2n)^{80}\text{Kr}$  reaction. The methods employed are standard techniques used in in-beam  $\gamma$ -ray spectroscopy. Earlier studies of nuclei in the  $A=70$  region have revealed several band structures including ground-state bands, additional positive-parity bands, negative parity bands, gamma bands, irregularities in the moment-of-inertia plots for the yrast bands, evidence for deformation, and the coexistence of nearly spherical and deformed shapes in the same nucleus. These studies are summarized in Refs. 1 and 2. Earlier rotation-aligned-model (RAL) calculations<sup>3-8</sup> had shown that the  $g_{9/2}$  orbital plays a special role for  $28 < N$ ,  $Z < 40$  in explaining the break in the moment-of-inertia plot of the yrast band and the nature of negative-parity bands. In this model, the strong Coriolis forces decouple two particles near the Fermi level in high  $j$  and low  $\Omega$  orbitals, and align their angular momenta with the rotational angular momentum of the core. The Coriolis interaction is maximum for particles in the valence shell  $(p_{3/2}, f_{5/2}, p_{1/2}, g_{9/2})$ . If the  $g_{9/2}$  orbital is sufficiently close to the Fermi energy, one expects several excited odd-parity and even-parity bands. The present paper deals with the details of our experimental results and the two-quasiparticle-plus-rotor calculations for  $^{80}\text{Kr}$ .

Earlier studies of  $^{80}\text{Kr}$  following  $\beta^-$  decay,<sup>9</sup> the  $(\alpha, Xn)$  reaction,<sup>10</sup> and Coulomb excitation are summarized in Ref. 11. Our preliminary results<sup>12</sup> on  $^{80}\text{Kr}$  appeared simultaneously with those of Funke *et al.*<sup>13</sup> In that paper,<sup>12</sup> we reported two  $8^+$  states, a second  $10^+$  state, and an additional  $12^+$  state in the yrast band that were not reported by Funke *et al.*<sup>13</sup> We attributed the break at  $8^+$  in the moment-of-inertia plot to the crossing of a band built on a two quasiparticle  $(g_{9/2})^2$  state with the ground-state band. We also reported several weak transitions between the gamma band and the ground-state band that agree with those in the latest decay scheme of Funke *et al.*<sup>14</sup> Our results are also in agreement with the low-lying level structure following proton induced reactions reported by Yoshikawa *et al.*<sup>15</sup>

Since several odd-odd and even-even transitional nuclei were satisfactorily described in terms of a quasiparticle-plus-rotor model,<sup>4-8</sup> we have used this model to calculate the levels in  $^{80}\text{Kr}$ . Our calculations indicate that the  $g_{9/2}$  orbital is playing an important role in this mass region.

### II. EXPERIMENTAL PROCEDURES AND RESULTS

The  $^{80}\text{Kr}$  nuclei were produced by the  $^{70}\text{Zn}(^{12}\text{C}, 2n)$  reaction with 33.0–38.4-MeV carbon ions extracted from the Oak Ridge National Laboratory ORNL EN tandem accelerator. A target of 0.25 mm thickness on a Ni backing and enriched up to 80% was used for the present studies. The target

thickness was just sufficient to stop the recoil nuclei. Angular distributions,  $\gamma$ - $\gamma$  coincidences, and  $\gamma$ - $\gamma$  directional correlation measurements were performed at a beam energy of 38.4 MeV. The  $\gamma$  rays were observed with Ge(Li) detectors of resolution 2.5 keV at 1.33 MeV and efficiencies of 18% of a 7.6 cm $\times$ 7.6 cm NaI detector.

The singles  $\gamma$ -ray spectrum from the  $^{70}\text{Zn}(^{12}\text{C}, 2n)^{80}\text{Kr}$  reaction at 55° with respect to the beam direction is shown in Fig. 1. The strong  $\gamma$  rays of  $^{80}\text{Kr}$  are labeled with energies in keV. Because of other isotopes of zinc present in the target, the  $\gamma$ -ray spectrum is very complex, and one clearly sees in Fig. 1 contamination lines from other reaction channels. The  $\gamma$ - $\gamma$  coincidence measurements were performed with two Ge(Li) detectors positioned at 0° and 90° with respect to the beam direction, the target to detector distance being 5 cm. The coincidence events were stored on a CDC 3200 computer through the buffer memory of a PDP 11 computer as a 1024  $\times$  1024 matrix. The coincidence spectra were obtained by setting windows on about 100 peaks and on their neighboring background regions. Selected coincidence spectra

are shown in Fig. 2.

The energy levels of  $^{80}\text{Kr}$  as deduced from our coincidence studies are summarized in Fig. 3. The energies and relative intensities for each transition are also given in Fig. 3. The errors are less than 5% for relative intensities greater than 10 and up to 20% for the weaker transitions.

Gamma-ray angular distribution measurements  $\gamma(\theta)$  were made at 0°, 55°, and 90° relative to the incident beam direction. A second Ge(Li) detector was placed at 135° to serve as a monitor for normalization purposes. The current integrator values measured using the target assembly as a Faraday cup were also used for the same purpose. In order to extract the angular distribution coefficients  $A_k$ , the experimental data were fitted to the polynomial

$$W(\theta) = 1 + \sum_{k=2,4} Q_k A_k P_k(\cos \theta),$$

where  $W(\theta)$  is the normalized  $\gamma$ -ray intensity at the angle  $\theta$  with respect to the beam direction, and  $Q_k$  is the solid angle correction. The angular distribution coefficients and  $\sigma/J$  are summarized

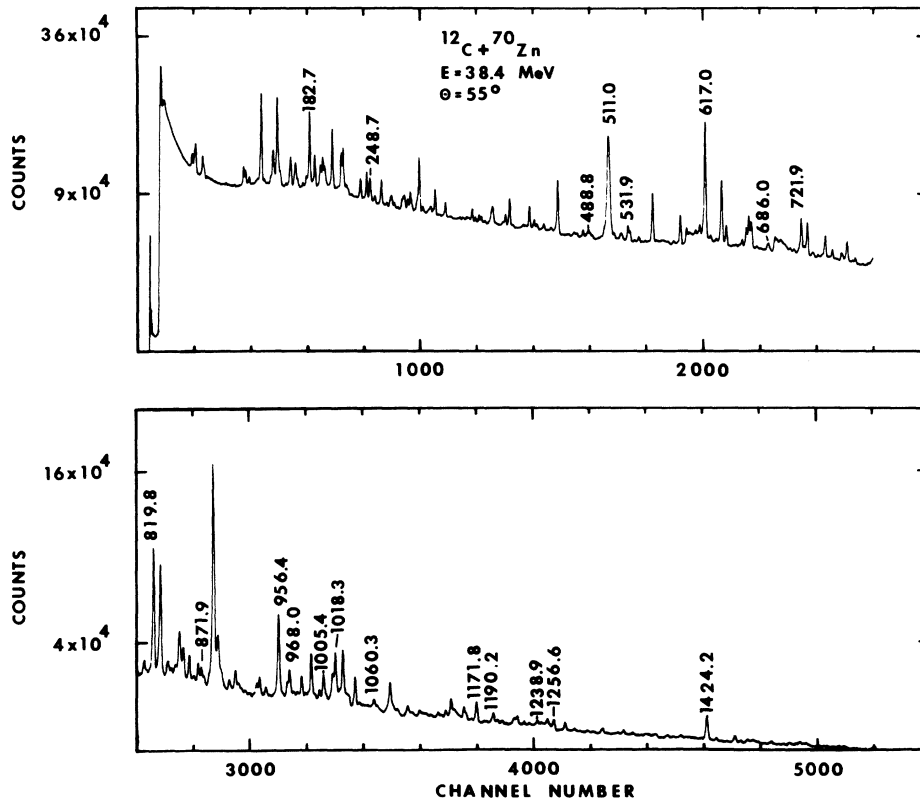


FIG. 1. Singles gamma ray spectrum from the  $^{70}\text{Zn}(^{12}\text{C}, 2n)$  reaction at a beam energy of 38.4 MeV. Energies in keV are given above the peaks for the strong  $\gamma$  rays of  $^{80}\text{Kr}$ .

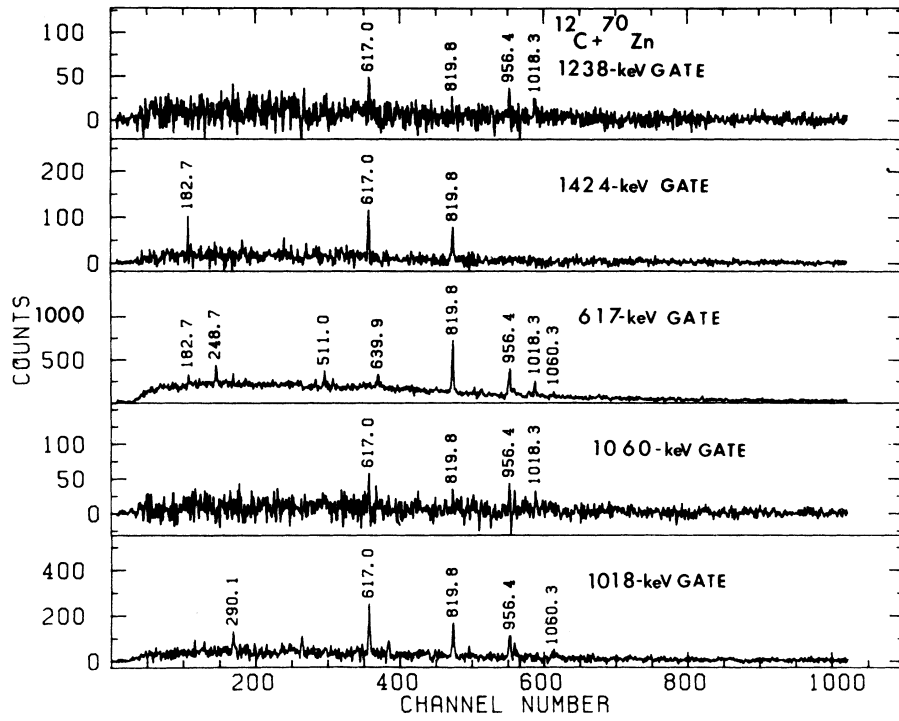


FIG. 2. Selected coincidence spectra corrected for background.

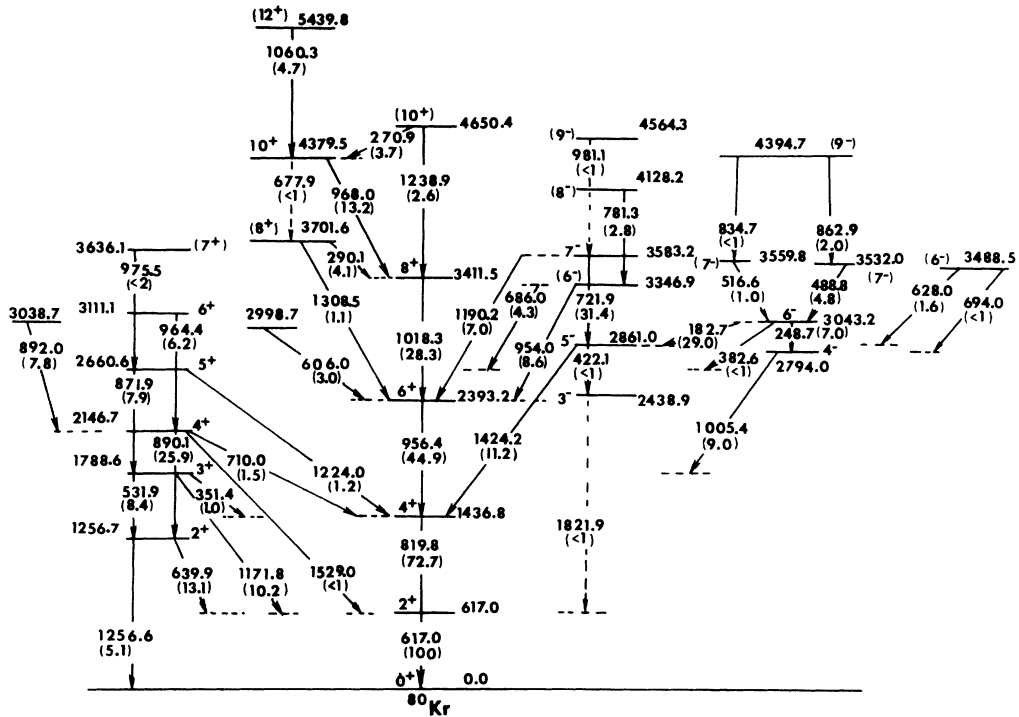


FIG. 3. The energy level diagram of <sup>80</sup>Kr obtained from the present experiment. The relative intensities are given in parentheses.

in Table I. The Gaussian width  $\sigma$ , for the population for magnetic substates  $m$  was defined by assuming the Gaussian model.<sup>16</sup> The spin sequence assumed in each case is also given in Table I.

Directional-correlation-from-oriented-nuclei (DCO) ratios were extracted from the  $\gamma$ - $\gamma$  coincidence experiment. The experimental DCO ratio is defined as  $R = W(90^\circ, 0^\circ)/W(0^\circ, 90^\circ)$ , where the two angles refer to the first and second members of the  $\gamma$ -ray cascade for the respective choice of angles. The theoretical DCO ratios were calculated with  $\alpha_2$ ,  $\alpha_4$ , and  $\delta$  ( $E2/M1$  admixture) obtained from the angular distribution measurement. The experimental and theoretical DCO ratios are given in Table II.

We have measured  $\gamma$ -ray yields at three projectile energies of 33.5, 35.5, and 38.4 MeV. Spin assignments could be made to some levels based on these yields. Only those spin values consistent with  $\gamma(\theta)$ , DCO ratio and yields measurements are shown in Table III.

### III. LEVELS AND SPIN PARITY ASSIGNMENTS

Most of the information about the levels of  $^{80}\text{Kr}$  is known only from the present study and the simultaneous work of Funke *et al.*<sup>14</sup> We introduced 29 levels in the decay scheme from a study of coincidence relationships. Many of the negative-parity states reported in Ref. 14 could not be verified in this experiment, presumably because the levels were either weakly populated or not populated in our reaction.

Of the 29 levels in  $^{80}\text{Kr}$  deduced from the present analysis, spin-parity assignments for 17 levels were made on the basis of (1) known systematics, (2) prior knowledge of the lower level spin, and

(3)  $\gamma(\theta)$ , DCO ratio, and yield measurements. The highest member of the yrast band at an energy of 5439.8 keV is assigned a  $12^+$  on the basis of coincidence intensities of the lower members of this band and systematics.

### IV. TWO-QUASIPARTICLE-PLUS-ROTOR MODEL CALCULATIONS

In the level structure of the  $^{80}\text{Kr}$  nucleus (Fig. 3), one can easily see the following four types of bands: (1) the ground-state band (GSB), (2) an excited positive-parity band, (3) an excited negative-parity band, and (4) a  $\gamma$ -vibrational-like band. The identification of the negative-parity band built on the  $5^-$  level at 2861.0 keV is based on the similarities in  $^{76}\text{Kr}$  and on  $^{78}\text{Kr}$  and the  $B(E2)$  values in Ref. 14. Previously, we have interpreted the excited positive-parity and negative-parity bands in the framework of the two-quasiparticle-plus-rotor model.<sup>6,7</sup> In the case of  $^{80}\text{Kr}$ , the high spin orbitals for protons and neutrons near the Fermi energy are  $g_{9/2}$  and  $f_{5/2}$ . One can interpret the excited positive-parity band, with a band head at  $8^+$ , as the alignment of two  $(g_{9/2})^2$  particles with the rotation axis, and the excited negative-parity band as the alignment of a  $g_{9/2}$  particle and a  $f_{5/2}$  particle with the rotation axis. We have performed two-quasiparticle-plus-rotor calculations for  $^{80}\text{Kr}$ , similar to those performed for the  $^{68}\text{Ge}$  nucleus.<sup>7,8</sup> The theory of two-quasiparticle-plus-rotor calculations has been described by Flaum and Cline.<sup>4</sup> These calculations have been modified by Samuelson *et al.*<sup>17</sup> to include the variable-moment-of-inertia (VMI) model features of Mariscotti, Scharff-Goldhaber, and Buck.<sup>18</sup> The following parameters are required for the necessary theoretical com-

TABLE I. Results of  $\gamma(\theta)$  measurements.

$E_\gamma$ (MeV)	$A_2$	$A_4$	$J_i \rightarrow J_f$	$\alpha_2$	$\alpha_4$	$(\sigma/J)_2$	$(\sigma/J)_4$
617.0	0.27(1)	-0.07(7)	2 $\rightarrow$ 0	0.38(1)	0.04(1)	0.64(1)	0.64(3)
819.8	0.32(1)	-0.09(1)	4 $\rightarrow$ 2	0.62(2)	0.24(3)	0.41(2)	0.40(2)
956.4	0.30(1)	-0.10(1)	6 $\rightarrow$ 4	0.65(3)	0.39(6)	0.38(2)	0.32(3)
1018.3	0.32(1)	-0.15(1)	8 $\rightarrow$ 6	0.76(3)	0.76(7)	0.30(2)	0.17(3)
968.0	0.22(2)	-0.13(2)	10 $\rightarrow$ 8	0.52(4)	0.73(10)	0.45(3)	0.18(4)
290.1	0.31(7)	-0.10(7)	8 $\rightarrow$ 8	0.57(9)		0.42(4)	
1256.7	0.45(3)	-0.15(4)	2 $\rightarrow$ 0	0.64(4)	0.09(2)	0.43(3)	0.51(4)
721.9	0.30(6)	-0.11(1)	7 $\rightarrow$ 5	0.68(1)	0.49(3)	0.35(1)	0.27(2)
248.7	0.26(1)	-0.16(1)	6 $\rightarrow$ 4	0.58(2)	0.64(5)	0.42(2)	0.22(3)
890.1	0.33(1)	-0.06(1)	4 $\rightarrow$ 2	0.64(2)	0.15(2)	0.39(1)	0.47(1)
871.9	0.44(2)	-0.22(2)	5 $\rightarrow$ 3	0.93(4)	0.77(7)	0.16(5)	0.17(3)
1238.9	0.22(4)	0.08(4)	10 $\rightarrow$ 8	0.53(9)	0.46(24)	0.44(6)	0.49(3)
1005.4	-0.16(4)	0.04(4)	4 $\rightarrow$ 3	0.44(12)		0.54(1)	
1424.2	-0.19(1)	-0.01(14)	5 $\rightarrow$ 4	0.57(4)		0.43(4)	
1171.8	0.29(2)	0.18(3)	3 $\rightarrow$ 2	0.50(3)		0.51(2)	

TABLE II. Experimental and theoretical DCO ratios of  $\gamma$  rays from  $^{80}\text{Kr}$ .

$E_{\gamma_1}$ (keV)	$E_{\gamma_2}$ (keV)	$R_{\text{exp}}$	Spin sequence	$R_{\text{cal}}^a$
819.8	617.0	0.98(6)	4 $\rightarrow$ 2 $\rightarrow$ 0	1.00
956.4	819.8	0.99(12)	6 $\rightarrow$ 4 $\rightarrow$ 2	1.00
1018.3	956.4	0.98(7)	8 $\rightarrow$ 6 $\rightarrow$ 4	1.00
968.0	1018.3	1.09(27)	10 $\rightarrow$ 8 $\rightarrow$ 6	1.00
290.1	1018.3	0.74(30)	8 $\rightarrow$ 8 $\rightarrow$ 6	0.88
248.7	1005.4	0.78(20)	6 $\rightarrow$ 4 $\rightarrow$ 3	0.55
1171.8	617.0	1.00(32)	3 $\rightarrow$ 2 $\rightarrow$ 0	0.92
639.9	617.0	1.88(23)	2 $\rightarrow$ 2 $\rightarrow$ 0	1.84 <sup>b</sup>
890.1	639.9	0.80(25)	3 $\rightarrow$ 2 $\rightarrow$ 2	0.929 <sup>b</sup>

<sup>a</sup> Calculated using  $\alpha_2$  and  $\delta$  values from angular distribution measurements.

<sup>b</sup> Calculated using a  $\delta$  value of  $-0.5$  for the 639.3 keV transition.

putations: (1)  $\delta$  deformation parameter, obtained from the  $B(E2)$  value of the  $2^+ \rightarrow 0^+$  transition; (2) the gap energy  $\Delta$ , which is approximately equal to  $12/A^{1/2}$  MeV, but can deviate considerably; (3) the Fermi energy  $\lambda$ , obtained from the Nilsson-type deformed-shell-model calculation; and (4) the two VMI parameters  $\vartheta_0$  and  $c$ .

As a first step in the computations, the one particle Nilsson wave functions for a series of  $\delta$  values were obtained to deduce the Nilsson diagrams for protons and neutrons. Once the value of  $\delta$  is known experimentally, the Fermi energy for both protons and neutrons can be obtained from the corresponding Nilsson diagrams. We need four different Nilsson calculations with the oscillator quantum number  $N=3$  and  $N=4$  for protons and neutrons in order to select the two-quasiparticle basis wave functions for even-parity and odd-parity bands. Our calculations indicate that the two-quasineutron states are higher in energy by 0.5–1.0 MeV than the two-quasiproton states. Hence, we present here the details of our two-quasiparticle-plus-rotor calculations for two-quasiproton bands. The shell model parameters<sup>19</sup>  $\kappa$  and  $\mu$  together with the values of  $\delta$  and  $\Delta$  are given in Table IV. The value of  $\delta$  is taken from Ref. 14. The VMI fit to the GSB is shown in Fig. 4. Our placement of the  $10^+$  level at 4650.4 keV in the GSB is based on the VMI prediction. The present placements of this level and the  $12^+$  level, in the GSB and the excited band, respectively, differ from those of Funke *et al.*<sup>14</sup>

The two-quasiparticle antisymmetrized wave functions were then constructed with the following as the basis states: for negative-parity states,  $\frac{5}{2}^-(422)$ ,  $\frac{3}{2}^-(431)$ ,  $\frac{1}{2}^-(440)$ ,  $\frac{7}{2}^-(303)$ ,  $\frac{5}{2}^-(312)$ ,  $\frac{1}{2}^-(310)$ ,  $\frac{3}{2}^-(312)$ , and  $\frac{1}{2}^-(321)$ , and for positive-parity states,  $\frac{9}{2}^+(404)$ ,  $\frac{7}{2}^+(413)$ ,  $\frac{5}{2}^+(422)$ ,  $\frac{3}{2}^+(431)$ ,  $\frac{1}{2}^+(440)$ . Two

TABLE III.  $\gamma$ -ray transition and level properties in  $^{80}\text{Kr}$ .

$E_{\text{level}}$ (keV)	$E_{\gamma}$ (keV)	$E/M$	Adopted ( $J^{\pi}$ )
617.0	617.0	$E2$	$2^+$
1256.7	1256.6	$E2$	$2^+$
1256.7	639.9	$M1 + E2$ ( $\delta = -0.5$ )	$2^+$
1436.8	819.8	$E2$	$4^+$
1788.6	1171.8	$M1 + E2$ ( $\delta = 0.5$ )	$3^+$
2138.9	1821.9		$3^-$ <sup>b</sup>
2146.7	890.1	$M1$	$4^+$
2393.2	956.4	$E2$	$6^+$
2660.6	871.9	$M1$	$5^+$
2794.0	1004.5	$E1$	$4^-$
2861.0	1424.2	$E2$	$5^-$
3043.2	248.7	$E2$	$6^-$
3111.1	964.4		$6^+$ <sup>a</sup>
3346.9	956.0		$6^-$ <sup>a</sup>
3411.5	1018.3	$E2$	$8^+$
3488.5	694.0		$(4^-)$ <sup>a</sup>
3532.0	488.8		$(7^-)$ <sup>a</sup>
3559.8	516.6		$7^-$ <sup>a</sup>
3583.2	721.9	$E2$	$7^-$
3636.1	975.5		$7^+$ <sup>a</sup>
3701.6	290.1	$M1 + E2$ ( $\delta = 0.3$ )	$8^+$
4379.5	968.0	$E2$	$10^+$
4394.7	834.7		$(9^+)$ <sup>a</sup>
4564.3	981.1		$9^-$ <sup>a</sup>
4650.4	1238.9	$E2$	$10^+$
5439.8	1060.3	$E2$	$12^+$

<sup>a</sup> From Ref. 14.

<sup>b</sup> From Ref. 24.

independent calculations were performed for even and odd two-quasiproton states. The Coriolis matrix elements between different basis states, final energies, and wave functions are obtained by matrix diagonalization.

The results of the calculated energies are compared to the experimental energies in Fig. 5. We have used the energy value of the  $14^+$  level of Ref. 14 in the comparison.

The positive-parity band built on the second  $8^+$  level at 3701.6 keV is an aligned band with a  $g_{9/2}$  configuration. For the negative two-quasiproton

TABLE IV. Shell model parameters used in the two-quasiproton-plus-rotor model calculations.  $\delta = 0.26$ ,  $\Delta(\text{gap}) = 0.65$ .

$N$	$\kappa$	$\mu$	Fermi energy ( $\lambda$ ) MeV
4	0.07	0.38	42.01
3	0.07	0.31	42.01

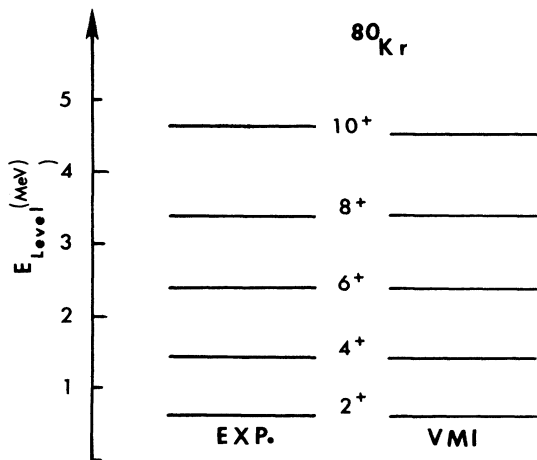


FIG. 4. Energy levels calculated by a VMI fit to the zero-quasiparticle band compared with experimental levels.

states, one particle occupies a  $g_{9/2}$  Nilsson orbital and the other a  $p_{3/2}$ ,  $f_{5/2}$ , or  $f_{7/2}$  Nilsson orbital. However, the proton Fermi energy lies close to the  $\Omega = \frac{1}{2}$  of  $f_{5/2}$  parentage and the  $\Omega = \frac{1}{2}$  of  $p_{3/2}$  parentage. The calculations show that nearly 90% of the contribution to the levels of odd-parity bands comes from the coupling of  $g_{9/2}$  and  $f_{5/2}$  protons with  $\Omega = \frac{1}{2}$  and  $\Omega = \frac{3}{2}$ . The  $\Delta J = 1$  negative-parity band built on the  $5^-$  state at 2861.1 keV shown in Fig. 3 could be due to the partial alignment of these states with the rotational axis of the weakly deformed core.

Arima and Iachello<sup>20</sup> have proposed an interacting-boson-approximation (IBA) model which provides a unified description of collective nuclear states in terms of a system of interacting bosons. We performed such calculations for the case of  $^{80}\text{Kr}$ , and the results were well reproduced when compared to experiment and are consistent with

those reported in Ref. 21. These calculations also justify our placing of the 4650.0 keV,  $10^+$  level in the zero-quasiparticle band, in contrast to that of Ref. 14.

## V. DISCUSSION

Of the four bands observed in  $^{80}\text{Kr}$  (Fig. 3), the GSB, the gamma band, and the negative-parity band are also seen in  $^{76}\text{Kr}$  (Ref. 22) and  $^{78}\text{Kr}$ ,<sup>23</sup> while the band built on the second excited  $8^+$  level is not. The  $3^-$  state at 2438.9 keV has been shown to be of octupole vibrational character,<sup>9,24</sup> and is therefore not thought to have strong single-particle parentage. A moment-of-inertia plot of the GSB and the band built on the second  $8^+$  level is shown in Fig. 6. One sees an interesting break at  $8^+$  followed by a back bending to the  $10^+$  level and finally a forward bending to the  $12^+$  level. This is in contrast to  $^{78}\text{Kr}$ ,<sup>23</sup> for which the break occurs at  $10^+$ . The anomalous structure in the moment-of-inertia plot is attributed to the crossing of the GSB and a rotation-aligned band built on the ( $8^+$ ) level at 3701.6 keV. Such an interpretation is supported by our two-quasiproton-plus-rotor calculations which were presented above. The difference in the occurrence of the break in the moment-of-inertia plots in  $^{80}\text{Kr}$  and  $^{78}\text{Kr}$  is ascribed<sup>1</sup> to the fact that the two-quasiparticle  $8^+$  state is at a higher excitation energy in the case of  $^{78}\text{Kr}$ . The cranked-shell-model calculations<sup>14</sup> also show that the two-quasiproton excitations play an important role in describing the level structure of  $^{80}\text{Kr}$ . The first  $2^+$  excited state in  $^{80}\text{Kr}$  occurs at a higher excitation energy (617 keV) than those in  $^{76}\text{Kr}$ (424 keV) and  $^{78}\text{Kr}$ (455 keV). The VMI-model calculations of the GSB yielded a smaller value for the moment of inertia of  $^{80}\text{Kr}$  than they did for that of  $^{76,78}\text{Kr}$ .

An even-parity band with  $\Delta J = 1$ , based on the

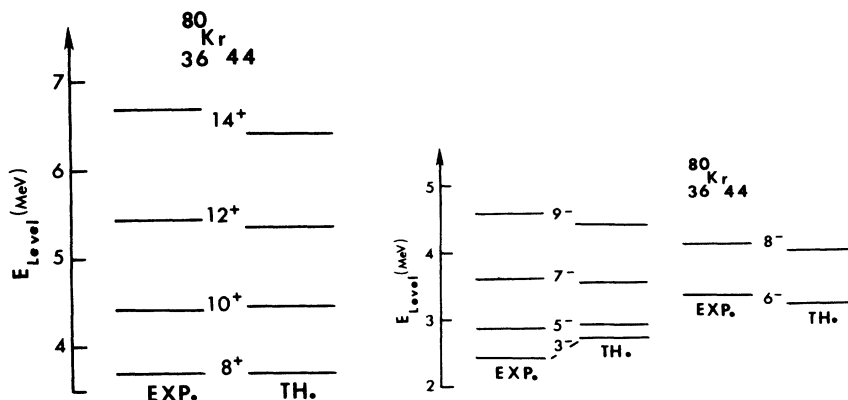


FIG. 5. Energy levels based on two-quasiparticle-plus-rotor-model calculations compared with experimental levels.

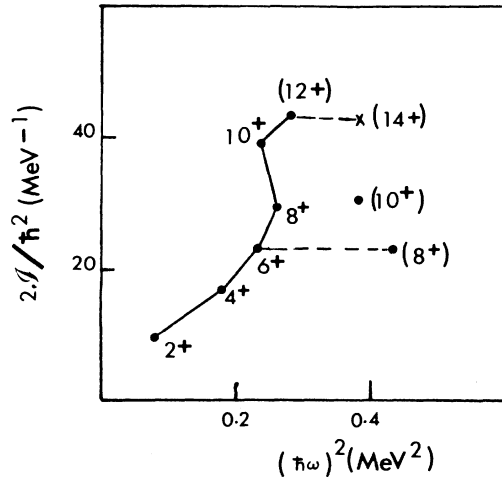


FIG. 6. Plot of the moment of inertia versus the rotational frequency squared for the even-spin yrast band. The point labeled X is from Ref. 14.

$2^+$  level at 1256.7 keV, is observed (Fig. 3). This band, and similar bands seen in  $^{76,78}\text{Kr}$ ,<sup>22,23</sup> have several common features characteristic of  $\gamma$ -vibrational bands found in well-deformed nuclei. The states decay primarily by  $\Delta J=2$  stretched- $E2$  transitions, and the interband transitions to the ground band are generally weak.

Figure 7 is an angular-momentum plot,<sup>25</sup> in which the intermediate spin  $J$  is plotted versus half of the  $\gamma$ -ray energy ( $\hbar\omega$ ), where  $\omega$  is the nuclear rotational frequency. If  $i_\alpha(\omega)=0$  for the GSB, then in the aligned band the nucleus has two aligned particles coupling to  $i_\alpha(\omega)=j$ . Experimentally,  $i_\alpha(\omega)$  is the difference in angular momentum between that of the band of interest and the GSB at a given frequency. A value of  $i_\alpha(\omega)\simeq 4$  is obtained for the  $5^-$  band, thus suggesting that the two quasiprotons are not fully aligned. A value of  $i_\alpha(\omega)\simeq 0$  is obtained for the even-parity and odd-parity spin members of the  $\Delta J=1$  band; this is consistent with the  $\gamma$ -vibrational character of this band. It is interesting to note that  $i_\alpha(\omega)$  for the two-quasiparticle  $8^+$  band, which involves two  $g_{9/2}$  particles, is the same as for the  $5^-$  band. However, Peker, Rasmussen, and Hamilton<sup>26</sup> have pointed out that reductions in alignment of the super band compared

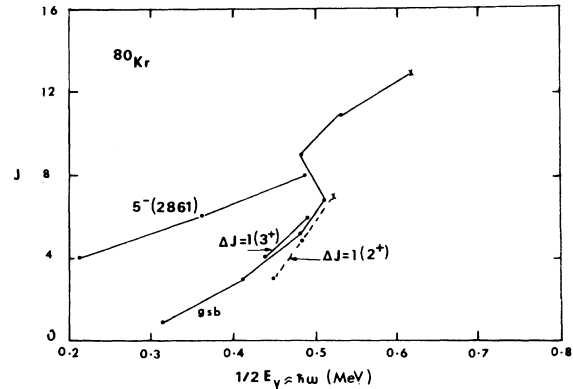


FIG. 7. Bohr and Mottelson angular momentum plots. The points X are from Ref. 14. The  $\Delta J=1(2^+)$  and  $\Delta J=1(3^+)$  plots are, respectively, from even-spin and odd-spin members of the  $\Delta J=1$  band.

to the ground band can occur when there is a strong mixing of the two bands. This may be the explanation for the small alignment of the  $8^+$  band.

## VI. SUMMARY

The level scheme of  $^{80}\text{Kr}$  reveals four strongly populated bands: three of positive parity and one of negative parity. The VMI model describes the ground-state band satisfactorily. The excited bands built on the second  $8^+$  and lowest  $5^-$  levels are well reproduced by two-quasiproton-plus-rotor model calculations. The break in the moment-of-inertia plot is attributed to the crossing of the ground-state band and the band built on the  $8^+$  state. The  $\Delta J=1$  band built on the second  $2^+$  state at 1256.7 keV is found to be of the  $\gamma$ -vibrational type. In general, the primary features of the  $^{80}\text{Kr}$  nucleus are understood in terms of the interaction of collective and single-particle degrees of freedom.

## ACKNOWLEDGMENTS

The research at Vanderbilt University was supported by the U.S. Department of Energy under Contract No. DE-AS0534-ER0534, and at Oak Ridge National Laboratory through Contract No. W-7405-eng.-26 with Union Carbide Corporation.

\*On leave from Andhra University, Visakhapatnam, India.

† On fellowship from Libyan Government.

‡ On leave from the Institute for Nuclear Sciences, Tokyo, Japan.

§ On leave from Coimbra University, Portugal.

<sup>1</sup>J. H. Hamilton, R. L. Robinson, and A. V. Ramayya, in *Lecture Notes in Physics*, edited by B. A. Robson (Springer, New York, 1978), Vol. 92, p. 253; R. L. Robinson and J. H. Hamilton, *Memorias del Segundo Simposio de Fisica Nuclear* (Oaxtepeck, Mexico, 1979), p. 358.

- <sup>2</sup>A. V. Ramayya and J. H. Hamilton, International Summer School Proceedings on Heavy Ion Physics, Predeal, Romania, 1978, edited by A. Berinde, V. Ceausescu, and I. A. Dorobantu, p. 305.
- <sup>3</sup>F. S. Stephens and R. S. Simon, Nuclear Phys. A183, 257 (1972).
- <sup>4</sup>C. Flaum and D. Cline, Phys. Rev. 14, 1224 (1976).
- <sup>5</sup>H. A. Smith, Jr. and F. A. Rickey, Phys. Rev. C 14, 1946 (1976).
- <sup>6</sup>P. C. Simms, F. Rickey, and R. Popli, invited talk, in *Proceedings of International Conference on Band Structure and Nuclear Dynamics, New Orleans, 1980*, edited by A. L. Goodman, G. S. Goldhaber, A. Klein, and R. A. Sorensen (North-Holland, Amsterdam, 1980), p. 205.
- <sup>7</sup>A. P. de Lima, J. H. Hamilton, A. V. Ramayya, B. Von Nooijen, R. M. Ronningen, H. Kawakami, E. de Lima, R. L. Robinson, H. J. Kim, W. K. Tuttle, L. K. Peker, F. A. Rickey, R. Popli, A. J. Caffrey, and J. C. Wells, Jr., Phys. Lett. 83B, 43 (1979).
- <sup>8</sup>A. P. de Lima *et al.* Phys. Rev. C 23, 213 (1981).
- <sup>9</sup>*Table of Isotopes*, 7th ed., edited by C. M. Lederer and V. S. Shirley (Wiley, New York, 1978).
- <sup>10</sup>D. G. McCauley and J. E. Draper Phys. Rev. C 4, 475 (1971).
- <sup>11</sup>L. R. Greenwood, Nucl. Data Sheets 15, 289 (1975).
- <sup>12</sup>D. L. Sastry, A. Ahmed, A. V. Ramayya, R. L. Robinson, R. B. Piercey, J. H. Hamilton, C. F. Maguire, H. Kawakami, A. P. de Lima, H. J. Kim, and J. C. Wells, Jr., in *Proceedings of the International Conference on Nuclear Structure, Tokyo, 1977*, edited by T. Marumori (Physical Society of Japan, Tokyo, 1978); Phys. Rev. C 14, 301 (1976); in Proceedings on the Nuclear and Solid State Physics Symposium, Poona, India, 1977 (unpublished), 20B., p. 183.
- <sup>13</sup>L. Funke, J. Doring, F. Dubbers, P. Kemnitz, H. Strunsky, E. Will, G. Winter, V. G. Kiptilij, M. F. Kudojaror, I. Kh. Lemberg, A. A. Pasternak, and A. S. Mishin, in *Proceedings on the International Conference on Nuclear Structure, Tokyo, 1977*, edited by T. Marumori (Physical Society of Japan, Tokyo, 1978), p. 300; in *Proceedings of the International Symposium on High Spin Phenomena and Nuclear Structure*, edited by L. Funke (Academy of Science DDR, Rossendorf, Afk-336, Dresden, 1977), p. 14.
- <sup>14</sup>L. Funke, J. Doring, R. Dubbers, P. Kemnitz, E. Will, G. Winter, V. C. Kiptilij, M. F. Kudojarar, I. Kh. Lemberg, A. A. Pasternak, A. A. Mishin, L. Hildingsson, A. Johnson, and T. H. Lindvald (unpublished).
- <sup>15</sup>N. Yoshikawa, Y. Shida, O. Hashimoto, M. Sakai and T. Numao, Nucl. Phys. A327, 477 (1979).
- <sup>16</sup>T. Yamazaki, Nucl. Data A3, 1 (1967).
- <sup>17</sup>L. E. Samuelson, J. A. Grau, F. A. Rickey, and P. Simms (unpublished).
- <sup>18</sup>M. A. Mariscotti, G. Scharff-Goldhaber, and B. Buck, Phys. Rev. 178, 1864 (1969).
- <sup>19</sup>B. Reehal and R. Sorenson Phys. Rev. C 2, 819 (1970).
- <sup>20</sup>A. Arima, F. Iachello, and I. Talmi, Phys. Lett. 66B, 205 (1977); A. Arima and F. Iachello, Ann. Phys. (N. Y.) 99, 253 (1976); 111, 201 (1978).
- <sup>21</sup>U. Kaup, A. Gelberg, W. Gast, and P. Von Brentano, in *Structure of Medium-Heavy Nuclei*, Conference Series Number 49 (Institute of Physics, Bristol, 1980), p. 40.
- <sup>22</sup>R. B. Piercey, A. V. Ramayya, J. H. Hamilton, C. F. Maguire, R. L. Robinson, H. J. Kim, and J. C. Wells, Jr., in *Lecture Notes in Physics*, edited by B. A. Robson (Springer, New York, 1978), Vol. 92, p. 606.
- <sup>23</sup>R. L. Robinson, H. J. Kim, R. O. Sayer, W. T. Milner, R. B. Piercey, J. H. Hamilton, A. V. Ramayya, J. C. Wells, Jr., and A. J. Caffery Phys. Rev. C 21, 603 (1980).
- <sup>24</sup>S. Matsuki, N. Sakamoto, K. Ogimo, V. Kadota, V. Saito, V. Tamabe, M. Yasue, and V. Okuma Phys. Lett. (to be published).
- <sup>25</sup>A. Bohr and B. R. Mottelson, in Proceedings of the International Conference on Nuclear Structure, Tokyo, 1977 [J. Phys. Soc. Jpn. Suppl. 44, 157 (1978)]; Physics Today 32, 25 (1979).
- <sup>26</sup>L. K. Peker, J. O. Rasmussen and J. H. Hamilton, Phys. Lett. 91B, 365 (1980).